Adsorption 5, 7–13 (1999)


# Cluster-Mediated Water Adsorption on Carbon Nanopores

K. KANEKO, Y. HANZAWA, T. IIYAMA, T. KANDA AND T. SUZUKI
*Physical Chemistry, Material Science, Graduate School of Science and Technology, Chiba University, 1-33 Yayoi-cho, Inage-ku, Chiba 263-8522, Japan*

**Abstract.** The adsorption isotherms of water at 303 K and $N_2$ at 77 K on various kinds of porous carbons were compared with each other. The saturated amounts of water adsorbed on carbons almost coincided with amounts of $N_2$ adsorption in micropores. Although carbon aerogel samples have mesopores of the great pore volume, the saturated amount of adsorbed water was close to the micropore volume which is much small than the mesopore volume. These adsorption data on carbon aerogels indicated that the water molecules are not adsorbed in mesopores, but in micropores only. The adsorption isotherms of water on activated carbon having micropores of smaller than 0.7 nm in width had no clear adsorption hysteresis, while the water adsorption isotherms on micropores of greater than 0.7 nm had a remarkable adsorption hysteresis above $P/P_0 = 0.5$. The disappearance of the clear hysteresis for smaller micropores suggested that the cluster of water molecules of about 0.7 nm in size gives rise to the water adsorption on the hydrophobic micropores; the formation and the structure of clusters of water molecules were associated with the adsorption mechanism. The cluster-mediated pore filling mechanism was proposed with a special relevance to the evidence on the formation of the ordered water molecular assembly in the carbon micropores by in situ X-ray diffraction.

**Keywords:** water cluster, water adsorption, hysteresis, electron radial distribution function, activated carbon fibers, carbon aerogel

## 1. Introduction

The structure of water in a confined space has gathered much attention from chemistry, biology, and earth science. In particular, water adsorbed in carbon nanopores, which is a model of water confined in hydrophobic nanoenviroments, should have a general importance. However, even water adsorption on activated carbon having nanopores is not sufficiently elucidated. Here, we use the term of nanopores for both micropores and smaller mesopores. The adsorption isotherm of water on activated carbon has a sharp adsorption uptake accompanying a clear adsorption hysteresis at a medium or higher relative pressure range. McBain et al. associated this noticeable uptake with the capillary condensation (McBain et al., 1933). Dubinin et al. introduced the hydrophilic site concept in order to understand water adsorption isotherms on carbonaceous materials and put the question for the capillary condensation mechanism for the steep adsorption jump (Dubinin et al., 1955). We have used the Dubinin-Serpinsky analysis for the water adsorption isotherm on activated carbon, which presumes the cluster growth of water on the hydrophilic site and their merge with the rise of the relative pressure (Dacey and Evans, 1971; Kaneko et al., 1989). Both of the McBain's capillary condensation mechanism and Dubinin's hydrophilic site-associated mechanism have the picture based on liquid state of water adsorbed in the carbon nanopore without sufficient structural study. Furthermore, both mechanisms have ambiguous points and thereby we must study this old adsorption problem of water adsorption on activated carbon.

The preceding X-ray diffraction and small angle X-ray scattering studies suggested that the micrographitic structure of cellulose-based activated carbon fiber (ACF) varies with water adsorption in micropores (Kaneko et al., 1991; Fujiwara et al., 1991; Suzuki and

Kaneko, 1992). Recently Iiyama et al. applied in situ X-ray diffraction technique to water confined in carbon micropores, showing that water molecular assembly has a solid like structure even at 303 K with the aid of electron radial distribution function (ERDF) analysis (Iiyama et al., 1995; Iiyama et al., 1996a, 1996b). French group also reported the diffraction study on water-wetted carbon recently (Bellissent-Funel et al., 1996). This ERDF analysis was applied to $CCl_4$ in the carbon micropore, showing the validity of the approach and presence of a special structure in the appropriate pore system (Iiyama et al., 1996a, 1996b; Iiyama et al., 1997a, 1997b). The structure analysis of $CCl_4$ in the graphite slit pore was also examined by GCMC simulation (Suzuki et al., 1997). On the other hand, adsorption and desorption experiments of NO and water on ACF gave an evidence for formation of nanoclathrate compound of NO and water at 303 K and subatmospheric pressure, although formation of the bulk NO hydrate is estimated to need the high pressure of more than 100 MPa at 303 K (Fujie et al., 1995).

As the contribution of the dispersion force to the whole intermolecular interaction of water is only 24% and the intermolecular interaction cannot be described by the Lennard-Jones potential (Rigby et al., 1986), it is not easy to simulate the water molecular state in the nanopore. Müller et al. proposed a simple simulation model using a Lennard-Jones sphere for a water molecule to get a qualitative agreement with the experimental adsorption isotherm (Müller et al., 1996). Accordingly, it is necessary to rewrite the picture on water confined in the carbon nanopore. The new concept of the structural water in the hydrophobic nanopore should develop new adsorption-related processes in the different fields.

This paper describes the adsorption mechanism of water on activated carbon with the relevance to structural information on water molecular assembly in carbon nanopores (Iiyama et al., 1997a, 1997b).

## 2. Experimental Section

The following various kinds of activated carbons of considerably uniform pore structures were used. Four kinds of pitch-based activated carbon fiber (ACF) (PIT-5, PIT-10, PIT-20, and PIT-25), carbon aerogels (CA), and activated carbon aerogels (a-CA) (Hanzawa et al., 1996). PIT-10 was heated in air at 373–1173 K for 1 h; the PIT-10 heated at $T$ K is denoted by PIT-10-$T$ in this article. The weight losses in percent due to the heat-treatment at $T$ K were zero at 373 K, 7 at 573 K, 16 at 773 K, 22 at 873 K, 23 at 973 K, and 30 at 1173 K. The micropore structures were determined gravimetrically by $N_2$ adsorption at 77 K. The water adsorption and desorption isotherms were determined gravimetrically at 303 K. When the amount of adsorption is expressed by the volume per unit weight of the adsorbent, the bulk liquid density was used ($N_2$: 0.807 $g \cdot ml^{-1}$ at 77 K and water: 0.996 $g \cdot ml^{-1}$ at 303 K). The X-ray diffraction of water adsorbed in micropores of carbon samples at 303 K was measured at 143–303 K by the transmission method using an angle-dispersive diffractometer (MAC science) in the scattering parameter $s$ range of 0.7–12 $Å^{-1}$. The temperature of the sample was kept constant within $\pm 0.1$ K for 303 K and within $\pm 5$ K at 143–255 K. The differential adsorption energy of water on PIT-20 was measured at 303 K using a twin-type calorimeter (Tokyo Riko Co.) as described earlier (Wang and Kaneko, 1995).

## 3. Results and Discussion

### *3.1. Comparison of Water and $N_2$ Adsorption Isotherms*

$N_2$ adsorption isotherms of all ACFs were of Type I, although the $N_2$ adsorption isotherms of PIT-20 and PIT-25 had a linear increase until $P/P_0 = 0.4$ after a marked uptake in the low pressure region. All PIT-10 samples heated at different temperatures had the representative Type I isotherm. Of course the $N_2$ adsorption isotherm of ACF had no hysteresis. Figure 1 shows the $\alpha_s$-plots for $N_2$ adsorption isotherms of PIT-10 samples. All $\alpha_s$-plots have a clear upward swing below $\alpha_s = 0.5$, indicating the uniform small micropores. We determined the micropore volume, the surface area, and the average pore width with the aid of SPE-method using high resolution $\alpha_s$-plot (Kaneko and Ishii, 1992; Setoyama et al., 1998). The $N_2$ adsorption isotherms of CA and a-CA are different from Type I, as shown in Fig. 3 later. The $N_2$ adsorption isotherms have a characteristic adsorption hysteresis. Their hysteresis-loops are of Type H1, coinciding with the network structure of agglomerates of uniform spherical particles. The adsorption uptake of a-CA at the low pressure is quite great due to development of micropores. Hence, CA has mainly mesopores, whereas a-CA has both of micropores and mesopores. The SPE-method is quite effective for the accurate determination of the microporosity and mesoporosity. The structures of micropores

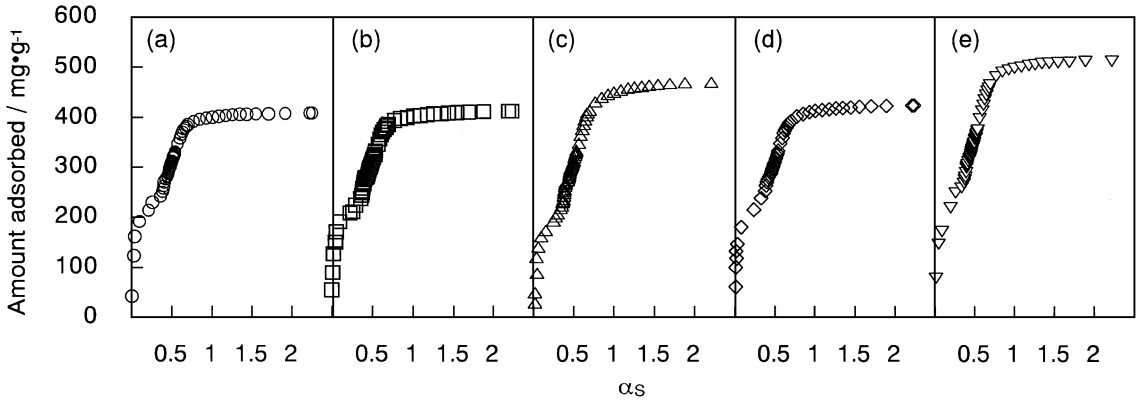


*Figure 1.* $\alpha_s$-plots for adsorption isotherms of nitrogen at 77 K based on the standard adsorption isotherm for nonporous carbon. (a) PIT-10-373, (b) PIT-10-573, (c) PIT-10-773, (d) PIT-10-973, and (e) PIT-10-1173.

and mesopores of carbon aerogel samples were separately determined. Table 1 lists the pore structures of all samples determined by the SPE method. All ACFs have only micropores, whereas CA and a-CA have both of uniform micropores and mesopores.

Figure 2 shows the water adsorption isotherms of PIT-10 heated at different temperatures. As PIT-10 was heated in air, basically the surface functional groups are produced by the heat-treatment. All water adsorption isotherms have a hysteresis, which varies from one sample to another. For all samples, the adsorption branch rises near $P/P_0 = 0.5$ as a usual case. On the contrary, the shape of the desorption branch is different from each other. The strong interaction of surface functional groups with adsorbed water should occur for PIT-10 samples heated at 573–973 K. A considerable adsorption uptake below $P/P_0 = 0.4$ supports the presence of the surface functional groups in these samples. The previous study (Kaneko et al., 1992) indicated that PIT-10-773 has the highest adsorption activity for $NH_3$ due to the greatest amount of surface carboxyl groups and the transformation of strong acidic functional groups to weak ones, e.g., ─COOH to ─OH occurs above 973 K. The change of the water adsorption hysteresis-shape reflects the variation of the surface composition of the carbon pores. Hence, the hydrophilic sites are essentially important in the adsorption hysteresis of water on activated carbon, as suggested by Dubinin et al. (1955). The saturated adsorption of water does not precisely agree with the micropore volume determined by $N_2$ adsorption (see Table 1). However, the ratio of the saturated water adsorption to the micropore volume is in the range of 0.82–1.17. Therefore, we can conclude that water molecules are adsorbed in micropores, considering the difficult determination of the saturated water adsorption and the ambiguous density of the adsorbed water in micropores.

*Table 1.* Micropore structures from $N_2$ adsorption at 77 K and saturated adsorption of water, $V_{H_2O}$, at 303 K.

| Sample | Surface area ($m^2\ g^{-1}$) | Pore volume ($ml\ g^{-1}$) | Pore width (nm) | $V_{H_2O}$ ($ml\ g^{-1}$) |
|---|---|---|---|---|
| PIT-10-373 | 1310 | 0.50 | 0.69 | 0.42 |
| PIT-10-573 | 1230 | 0.50 | 0.78 | 0.43 |
| PIT-10-773 | 1300 | 0.56 | 0.87 | 0.52 |
| PIT-10-973 | 1280 | 0.52 | 0.81 | 0.43 |
| PIT-10-1173 | 1510 | 0.62 | 0.83 | 0.52 |
| PIT-5 | 900 | 0.34 | 0.75 | 0.28 |
| PIT-20 | 1770 | 0.97 | 1.13 | 0.88 |
| PIT-25 | 1940 | 1.34 | 1.45 | 1.2 |
| CA | | | | |
| Micropores | 370 | 0.12 | 0.63 | 0.13 |
| Mesopores | 350 | 1.19 | 14 | |
| a-CA | | | | |
| Micropores | 1260 | 0.46 | 0.73 | 0.54 |
| Mesopores | 680 | 2.15 | 13 | |

Figure 3 shows the water adsorption isotherm of PIT-5 and PIT-20 at 303 K. The adsorption isotherm of PIT-20 has the steep rise at $P/P_0 = 0.7$ with a marked hysteresis, while the isotherm of PIT-5 rises near $P/P_0 = 0.5$ and it has a slight hysteresis. The uptake pressure of PIT-20 is higher than that of PIT-10 samples. The saturated adsorption of water for both samples is slightly smaller than the micropore volume,

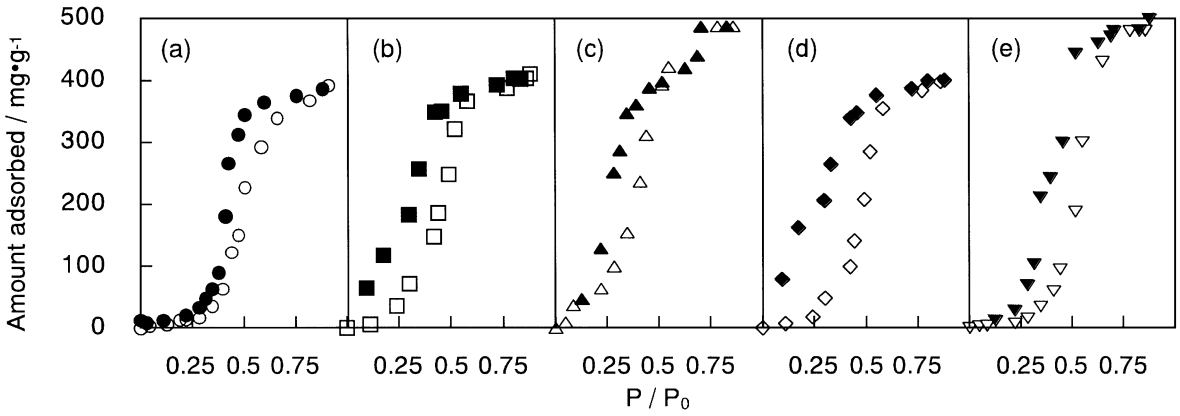


*Figure 2.* The adsorption isotherms of water on oxidized PIT-10 at 303 K. (a) PIT-10-373, (b) PIT-10-573, (c) PIT-10-773, (d) PIT-10-973, and (e) PIT-10-1173. Open and solid symbols denote adsorption and desorption branches, respectively.

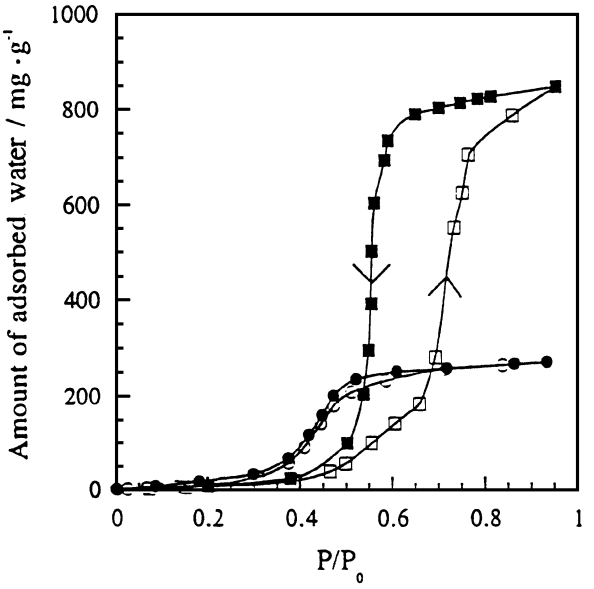


*Figure 3.* The adsorption isotherms of water on PIT-5 and PIT-20 at 303 K. (circle) PIT-5; (square) PIT-20. Open and solid symbols denote adsorption and desorption branches, respectively.

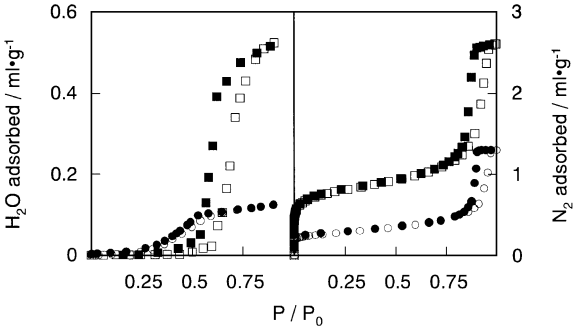


*Figure 4.* The adsorption isotherms of water at 303 K and $N_2$ at 77 K. (circle) CA; (square) a-CA. Open and solid symbols denote adsorption and desorption branches, respectively.

but water should be adsorbed in micropores regardless of the difference in the adsorption hysteresis. It is noteworthy that the water adsorption isotherm has almost no hysteresis in case of PIT-5. Although there is no sufficient surface functional groups on the micropore surface from the very slight adsorption below $P/P_0 = 0.4$ and the micropore surface is hydrophobic, the marked water adsorption begins at $P/P_0 = 0.4$ without the marked adsorption hysteresis. The Dubinin's hydrophilic site-associated mechanism is not enough for description of this result. The similar results were obtained in carbon aerogel samples.

As CA has uniform mesopores, water must condense in the mesopores if the capillary condensation mechanism is held. Figure 4 shows the water adsorption isotherms of CA and a-CA at 303 K. Their adsorption isotherms of $N_2$ are also shown in Fig. 4 for comparison. Both $N_2$ adsorption isotherms have a distinct hysteresis of Type H1, as described above. The condensation pressures predicted by the Kelvin equation for CA and a-CA using the cylinder model are $P/P_0 = 0.86$ and 0.85, respectively, agreeing with the observed value for both samples. Thus, $N_2$ molecules are adsorbed on mesoporous carbons mainly by capillary condensation mechanism, although a part of $N_2$ molecules are adsorbed in micropores. On the other hand, the water adsorption behavior is completely different from the $N_2$ adsorption. The adsorption isotherm of water on CA has a noticeable uptake near $P/P_0 = 0.5$

with a small hysteresis as well as PIT-5, whereas a-CA has a clear adsorption hysteresis. This difference in the adsorption hysteresis is similar to that of PIT-5 and PIT-20 in Fig. 3. The condensation pressures for water on mesopores of CA and a-CA calculated from the Kelvin equation are $P/P_0 = 0.85$ and 0.78, respectively, which are far from the observed values. Furthermore, the saturated water adsorptions of PIT-5 and PIT-20 are much smaller than those of total pore volumes. Approximately both saturated water adsorptions correspond to those of the micropore volume. Thus, water cannot be adsorbed on mesopores with the capillary condensation mechanism. Although apparent adsorption behaviors of water on activated carbons resemble capillary condensation of vapors on mesopores, water is not adsorbed on activated carbons with the capillary condensation.

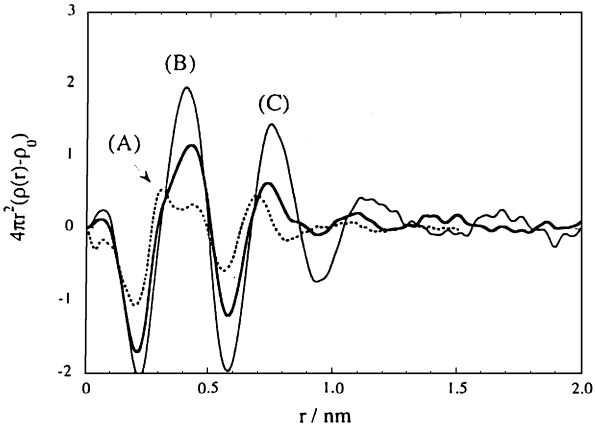


*Figure 5.* The electron radial distribution functions of water confined in micropores of PIT-5 and -10 and bulk liquid water at 303 K. Fine solid line: PIT-5, bold solid line: PIT-20, and dotted line: liquid water.

### *3.2. The Structure and State of Water in Carbonaceous Micropores*

Physical adsorption of vapors occurs on the flat or macropore surfaces with the multi-layer adsorption, on adsorbed multilayer-coated mesopores with the capillary condensation, and on micropores with micropore filling according to the IUPAC classification (Rouquerol et al., 1994). The classification was based on the $N_2$ adsorption. The molecular size of $H_2O$ is estimated to be 0.31 nm (Müller et al., 1996) or 0.36 nm (MacClellan and Harnsberger, 1967), which is close to that of $N_2$ (Lennard-Jones parameter: 0.363 nm, average thickness: 0.354 nm). Therefore, the classification of pores can be applied to water without any modification. We can conclude that water molecules are not adsorbed on mesopores by the capillary condensation mechanism, but adsorbed on only micropores by another mechanism.

Is water confined in micropores liquid? We have believed that not only water, but also other vapors are condensed in pores in the liquid state because of the goodness of the well-known Gurvitsch rule (Gregg and Sing, 1982). Figure 5 shows the electron radial distribution function (ERDF) of water adsorbed in micropores of PIT-5 and PIT-20 together with that of the bulk liquid water at 303 K. Figure 5 shows the explicit difference in the features of (A) at 0.35 nm, (B) at 0.42 nm, and (C) at 0.7 nm for three water systems. The (A) (shoulder in case of adsorbed water), (B), and (C) peaks are assigned to the nearest-neighbor, the second nearest-neighbor, and the third nearest neighbor water molecules, respectively. Hence, these peaks provide the detailed information on the short range structure of water molecular assembly in the micropore. As bulk liquid water has an interstitial molecule at the nearest-neighbor position, and thereby the peak (A) is higher than peak (B) in case of bulk liquid water. The comparison of the peaks (A) and (B) indicates the ordered state of water molecules. The ERDF of adsorbed water has only a shoulder at 0.35 nm, indicating the ordered structure of water in the micropores. Further, the higher peak of (B) is ascribed to the immobile state of water molecules. Hence, water adsorbed in micropores of PIT-5 has a more ordered and rigid structure than that of PIT-20. The ERDF changed as lowering the measuring temperature to 143 K for both samples. However, the change of the ERDF of water in the micropores of PIT-5 was only slight, whereas the ERDF of water in the micropores of PIT-20 at 143 K was close to that of PIT-5. The water molecular assembly has an ordered structure different from the bulk liquid. In particular, the narrower the pore width, the more ordered the water molecular assembly structure. Then, we must take into account this important ordering of water molecules in micropores.

The differential adsorption energy of water on PIT-20 at 303 K was 44 $kJ \cdot mol^{-1}$, which is almost equal to the enthalpy of liquefaction of water (43.6 $kJ \cdot mol^{-1}$). This result coincides with the earlier studies (McBain et al., 1933; Dubinin et al., 1955). Iiyama et al. reported that the molecular structure of adsorbed water of the fractional filling = 0.3 or 0.6 in the carbon micropore is more ordered than that of the fractional filling

$= 1$ (Iiyama et al., 1995). Accordingly the microscopic structure of the water molecular assembly is different from the bulk liquid, but the macroscopic state of water adsorbed in the micropore from the calorimetric study is quite similar to the bulk liquid. The enthalpy of fusion of bulk ice is only 6 $kJ \cdot mol^{-1}$, being much smaller than the enthalpy of liquefaction. We need the more careful determination of the differential adsorption energy of water in order to get an explicit difference between the confined water and bulk liquid one from the calorimetric study.

### *3.3. Cluster-Mediated Water Adsorption and the New Potential for Application*

It is well-known that water molecules form the dimer (Curtiss et al., 1979; Eisenberg and Kauzman, 1969). When the thermodynamic relation for the bulk gas phase is applied formally to liquid water at 303 K and 0.1 MPa and at 303 K and 10 MPa (regardless of unrealistic conditions), about 3 and 60% of molecules are dimerized, respectively. In the hydrophobic micropore, water molecules are expected to be more dimerized due to the compressed conditions. In the micropore the dimers grow to a greater cluster such as the pentamer $(H_2O)_5$, which has been used for the model of the elemental structure of water. The size of the pentamer is about 0.5 nm. Adachi calculated the electronic structure of the pentamer with the Discrete Variational $X_\alpha$ method, showing that the effective charges of the oxygen and hydrogen atoms in the water molecule increase in the pentamer compared with the monomer (Adachi, 1991). Therefore, the electrostatic charges should be more compensated in the pentamer than the monomer; the pentamer can be approximated by the neutral sphere upon interaction with the pore-wall. The more neutral pentamer may interact with the carbon micropore through the Lennard-Jones type interaction to be adsorbed, although we could not measure precisely the interaction yet. It is presumed that such pentamers are formed through the dimer in the micropore near $P/P_0 = 0.5$.

The water adsorption isotherms of PIT-5 and AC whose pore widths are less than 0.7 nm should be caused by the presence of the small micropore size. Recently Freeman et al. also reported that water adsorption isotherm low burn-off carbon shows a slight hysteresis (Freeman et al., 1995). Their results also indicate that the small pore is associated with the disappearance of the clear adsorption hysteresis. In case of the narrow micropore of the pore width $<0.7$ nm, water molecules form the clusters of the size of the pentamer which is roughly fit for the pore size. Both adsorption and desorption are based on the same cluster formation equilibrium and thereby the adsorption isotherm has no distinct hysteresis. On the other hand, water molecules form the structure having a longer range order in the micropore greater than about 1 nm in width through the cluster formation of such as the pentamer. Then the elementary equilibria of adsorption and desorption are different from each other, giving rise to the marked adsorption hysteresis. Although we have evidences in some aspects, we need the structural and energetic information on the fine structure of the cluster.

The question why water vapor is not adsorbed in mesopores by the capillary condensation is not explained by the above mechanism yet. In case of water adsorption on carbon mesopores, we must treat an adsorbed water as a continuos media and the contact angle of water to the carbon pore-wall should be taken into account. The contact angle of water on graphite is 86° (Adamson, 1990), and thereby the condensation pressure remarkably shifts to the higher value corresponding to the macropore size, that is, near to $P/P_0 = 1$. It is quite difficult to measure directly the capillary condensation of water on carbon mesopores near the saturated vapor pressure. Also the Saam-Cole analysis (De Keizer et al., 1991; Hanzawa et al., 1998), about adsorption on mesopores can give a useful information on adsorption of water on carbon mesopores.

## Acknowledgments

We acknowledge the Ministry of Education for the Grant-in-Aid for Scientific Research on Priority Area of Japanese Government (Carbon Alloys 09243102).

## References

Adachi, H., *Introduction to Quantum Material Chemistry* (Japanese), chap. 8, Sankyou Shuppan, Tokyo, 1991.

Adamson, A.W., *Physical Chemistry of Surfaces*, p. 397, Wiley Interscience, New York, 1990.

Bellissent-Funel, M.-C., R. Sridi-Dorbez, and L. Bosio, "X-Ray and Neutron Scattering Studies of the Structure of Water at a Hydrophobic Surface," *J. Chem. Phys.*, **104**, 10023–10029 (1996).

Curtiss, L.A., D.J. Frurip, and M. Blander, "Studies of Molecular Association in $H_2O$ and $D_2O$ Vapors by Measurement of Thermal Conductivity," *J. Chem. Phys.*, **71**, 2703–2711 (1979).

Dacey, J.R. and M.J. Evans, "Volume Changes in Saran Charcoal Caused by the Adsorption of Water, Methanol, and Benzene Vapors," *Carbon*, **9**, 579–585 (1971).

De Keizer, A., T. Michalski, and G.H. Findenegg, "Fluids in Pores: Experimental and Computer Simulation Studies of Multilayer Adsorption, Pore Condensation, and Critical-Point Shifts," *Pure Appl. Chem.*, **63**, 1495–1502 (1991).

Dubinin, M.M., E.D. Zaverina, and V.V. Serpinsky, "The Sorption of Water Vapour by Active Carbon," *J. Chem. Soc.*, **1955**, 1760–1766 (1955).

Eisenberg, D. and W. Kauzman, *The Structure and Properties of Water*, p. 53, Oxford University Press, London, 1969.

Freeman, J.J., J.B. Tomlinson, K.S.W. Sing, and C.R. Theocharis, "Adsorption of Nitrogen and Water Vapour by Activated Nomex® Chars," *Carbon*, **33**, 195–799 (1995).

Fujie, K., S. Minagawa, T. Suzuki, and K. Kaneko, "NO/$H_2O$ Clathrate Formation in Sub-Nano Graphitic Slit Space," *Chem. Phys. Lett.*, **236**, 427–430 (1995).

Fujiwara, Y., K. Nishikawa, T. Iijima, and K. Kaneko, "A Simulation Study of Small Angle X-Ray Scattering Behavior of Activated Carbon Fibers Adsorbing Water," *J. Chem. Soc. Faraday Trans.*, **87**, 2763–2768 (1991).

Gregg, S.J. and K.S.W. Sing, *Adsorption, Surface Area, and Porosity*, chap. 3, Academic Press, London, 1982.

Hanzawa, Y., K. Kaneko, R.W. Pekala, and M.S. Dresselhaus, "Activated Carbon Aerogels," *Langmuir*, **12**, 6167–6169 (1996).

Hanzawa, Y., N. Yoshizawa, K. Kaneko, R.W. Pekala, and M.S. Dresselhaus, "Pore Structure Determination of Carbon Aerogels," *Adsorption*, in press.

Iiyama, T., K. Nishikawa, T. Otowa, and K. Kaneko, "A Ordered Water Molecular Assembly in a Slit-Shaped Carbon Nanospace," *J. Phys. Chem.*, **99**, 10075–10076 (1995).

Iiyama, T., K. Nishikawa, T. Otowa, T. Suzuki, and K. Kaneko, "Organized Molecular States in Carbon Micropores," *Fundamentals of Adsorption*, M.D. LeVan (Ed.), pp. 401–408, Kluwer Academic Pub., MA, 1996a.

Iiyama, T., K. Nishikawa, T. Otowa, T. Suzuki, and K. Kaneko, "Molecular Assembly Structure of $CCl_4$ in Graphitic Nanospaces," *J. Phys. Chem. B*, **101**, 3037–3042 (1997a).

Iiyama, T., T. Nishikawa, T. Suzuki, and K. Kaneko, "Study of Structure of Water Molecular Assembly in a Hydrophobic Nanospace at Low Temperature with in situ X-Ray Diffraction," *Chem. Phys. Lett.*, **274**, 152–158 (1997b).

Iiyama, T., T. Suzuki, and K. Kaneko, "An Imperfect Packing of $CCl_4$ Molecules Confined in a Graphitic Slit Nanospace," *Chem. Phys. Lett.*, **259**, 37–40 (1996b).

Kaneko, K. and C. Ishii, "Superhigh Surface Area Determination of Microporous Solids," *Colloid Surf.*, **67**, 203–212 (1992).

Kaneko, K., T. Katori, K. Shimizu, N. Shindo, and T. Maeda, "Changes in the Molecular Adsorption Properties of Pitch-Based Activated Carbon Fibers by Air Oxidation," *J. Chem. Soc. Faraday Trans.*, **88**, 1305–1309 (1992).

Kaneko, K., N. Kosugi, and H. Kuroda, "Characterization of Iron Oxide Dispersed Activated Carbon Fibers with Water Adsorption and Fe K-Edge XANES and EXAFS," *J. Chem. Soc. Faraday Trans. I*, **85**, 869–881 (1989).

Kaneko, K., T. Suzuki, Y. Fujiwara, and K. Nishikawa, "Dynamic Micropore Structures of Micrographitic Carbons During Adsorption," *Characterization of Porous Solids II*, F. Rodriguez-Reinoso, J. Rouquerol, K.S.W. Sing, and K.K. Unger (Eds.), pp. 389–398, Elsevier, Amsterdam, 1991.

MacClellan, A.L. and H.F. Harnsberger, "Cross-Section Areas of Molecules Adsorbed on Solid Surface," *J. Colloid Interface Sci.*, **23**, 577–599 (1967).

McBain, J.W., J.L. Porter, and R.F. Sessions, "The Nature of the Sorption of Water by Charcoal," *J. Amer. Chem. Soc.*, **55**, 2294–2304 (1933).

Müller, E.A., L.F. Rull, L.F. Vega, and K.E. Gubbins, "Adsorption of Water on Activated Carbons: A Molecular Simulation Study," *J. Phys. Chem.*, **100**, 1189–1196 (1996).

Rigby, M., E.B. Smith, W.A. Wakeham, and G.C. Maitland, *The Forces between Molecules*, chap. 1, Oxford Sci. Pub., Oxford, 1986.

Rouquerol, J., D. Avnir, C.W. Fairbridge, D.H. Everett, J.H. Hynes, N. Pernicone, J.D.F. Ramsay, K.S.W. Sing, and K.K. Unger, "Recommendation for the Characterization of Porous Solids," *Pure Appl. Chem.*, **66**, 1739–1758 (1994).

Setoyama, N., T. Suzuki, and K. Kaneko, "Simulation Study on Relationship between High Resolution $\alpha_s$-Plot and Pore Size Distribution for Activated Carbon," *Carbon*, **36**, 1459–1467 (1998).

Suzuki, T. and K. Kaneko, "The Structural Change of Graphitization-Controlled Microporous Carbon upon Adsorption of $H_2O$ and $N_2$," *J. Chem. Soc. Faraday Trans.*, **88**, 1305–1309 (1992).

Suzuki, T., K. Kaneko, and K.E. Gubbins, "Pore Width-Sensitive Filling Mechanism for $CCl_4$ in a Graphitic Micropore by Computer Simulation," *Langmuir*, **13**, 2545–2549 (1997).

Wang, Z.-M. and K. Kaneko, "Dipole Oriented States of $SO_2$ Confined in a Slit-Shaped Graphitic Subnanospace from Calorimetry," *J. Phys. Chem.*, **99**, 16714–16721 (1995).